Responsive Glazing Systems: Characterisation Methods and Winter Performance

Nomenclature

C	thermal conductance (W/(m^{2}K))
E	specific energy (Wh/m^2)
Ev	vertical illuminance (lx)
H	specific incident daily solar radiation (kWh/m^2)
HF	monitored surface Heat Flux (W/m^2)
I	specific incident solar irradiance (W/m^2)
$\dot{q}$	specific heat flux (W/m^2)
t	time (h)
U	thermal transmittance (W/(m^{2}K))

Greek symbols

τ	transmittance (-)
ρ	reflectance (-)
ϑ	temperature (°C)

Superscripts

*	referred to an equivalent value
+	referred to heat flux/energy gain
-	referred to heat flux/energy loss

Subscripts

air	referred to air
average	referred to an average value
e	solar
ex	excursion
in	referred to the indoor environment
n	referred to normalised energy
out	referred to the outdoor environment
surf	referred to the surface
tot	total including long-wave and short-wave radiation
v	visible
24	referred to daily energy

Acronyms

HDD	Heating Degree Day
IR	Infrared
PMV	Predicted Mean Vote
TGU	Triple Glazing Unit, reference technology
TGU_TT	Triple Glazing Unit with thermotropic glazing
TGU_TT+PCM(IN)	Triple Glazing Unit with thermotropic glazing and a PCM-filled cavity in the inner position
TGU_TT+PCM(OUT)	Triple Glazing Unit with thermotropic glazing and a PCM-filled cavity in the outer position
TT	thermotropic glazing

Abstract

Responsive envelope components are promising technologies for improving the energy and indoor comfort performance of buildings. As far as the transparent envelope is concerned, several experimental and numerical researches have been carried out in recent years, focusing on the integration of Phase Change Materials (PCM) in glazing systems. To overcome some limitations highlighted during previous experimental campaigns, a new concept was prototyped, and the energy and comfort performance of a full-scale prototype was experimentally assessed in an outdoor test cell facility. In this paper, the focus is placed on the evaluation of the cold-season behaviour.

The proposed glazing system comprises a triple-glazed unit with a PCM-filled cavity and a thermotropic glass placed on the outer side. The thermotropic glass acted as a switchable shading system capable of regulating the phase transition of the PCM by modulating the amount of solar radiation impinging on the PCM layer. The thermophysical and optical behaviour of the technology was monitored with the PCM alternately placed in the inner or the outer cavity of the triple-glazed unit and compared against a reference triple-glazing unit. In parallel to the measurements on the glazing with PCM and thermotropic glass, a triple-glazed unit equipped with a thermotropic glass was also monitored, giving a total of three different glazing systems under analysis.

Representative days were selected in order to analyse the performance of the proposed technologies under significant and comparable boundary conditions. The equivalent thermal conductance of each technology was evaluated. The energy performance was assessed by means of both a long-term analysis and daily analyses on cloudy and sunny days. In addition, the visible transmittance of the three technologies was estimated through hourly measurements of vertical illuminance performed during a cloudy and a sunny day. Moreover, implications on thermal comfort conditions were evaluated ex-post by means of numerical simulations based on experimental data.

The results showed that, during cloudy winter days, the position of the PCM did not influence the overall performance of the prototype since it never changed phase. On the other hand, during sunny winter days, the glazing with the PCM in the outer position underwent phase transition and presented a slightly better performance.

Highlights:

- Two novel responsive windows were devised and tested in an outdoor test cell facility.
- A PCM-filled cavity and a thermotropic pane were integrated in a triple-glazed window.
- The thermotropic glazing was applied to regulate the phase transition of the PCM.
- Reference triple-glazed units with and without a thermotropic layer were also tested.
- Daily and long-term performance evaluations were carried out under winter conditions.

Keywords: window systems, responsive glazing, dynamic component, PCM, thermotropic glass, switchable glazing, experimental activity, energy performance, thermal comfort.

1 Introduction

1.1 Background

Glazing systems are key components of the building envelope, affecting the energy and environmental performance of buildings in several ways. On the positive side, they allow natural light to be exploited for daylighting; however, on the negative side, they are responsible for the largest component of heat gain and heat loss.

Due to the opposing requirements that arise during the different seasons (allow/reject solar gain, reduce heat loss, control light gain), the most promising direction of research and development for glazing technologies in the improvement of energy and indoor environmental performance is towards solutions that allow a dynamic behaviour to be achieved, as shown in a recent study on the energy-saving potential of an ideal dynamic glazed system (Favoino et al., 2015).

Several possibilities can be exploited to turn glazing systems into responsive and dynamic components. The integration of mechanical shading systems is probably the most popular option and, when combined with ventilated cavities, good performance can be achieved (including solar energy exploitation through the thermal energy of the ventilation flow).

Another approach is based on the adoption of active layers that modify the optical properties of the glazing, usually acting on the transmittance and absorptance of the layer (Baetens et al., 2010). Some of these technologies are based on self-triggered adaptive mechanisms (i.e. passive-dynamic, or responsive, technologies) or on a controllable external stimulus (i.e. active-dynamic technologies). Among the most investigated passive technologies, it is worth mentioning thermochromic, thermotropic, and photochromic layers. The most common active-dynamic technologies are electrochromic, light particle devices, and liquid crystal devices.

When focusing on responsive glazing technologies, thermochromic/thermotropic layers have been the most widely investigated and tested materials. While thermochromic materials present a dependency of the solar/visible absorption coefficient on the layer's temperature (the higher the temperature, the higher the absorption coefficient), thermotropic materials present different transmission modes depending on the temperature of the layer (direct-to-direct transmission occurs at low temperature levels, whereas at high temperature levels the diffuse transmission becomes dominant, and the total reflectivity of the layer increases).

Several authors studied thermotropic glazing with a focus on the material level. Muehling et al., (2009) presented the preparation and optical characterisation of a glass–resin–glass thermotropic system. Seeboth et al., (2010) reviewed materials and technologies for thermotropic and thermochromic glazing. Weber and Resch, (2012) studied the effect of material composition on the performance of thermotropic systems with fixed domains for overheating protection. Gladen et al., (2014) performed a parametric analysis to identify potential material combinations for manufacturing thermotropic glazing for application on flat plate solar collectors.

The optical and thermophysical performance of thermotropic systems has also been assessed by means of in-situ measurements (Raicu et al., 2002) and numerical simulation (Allen et al., 2017; Georg et al., 1998). In different investigations, the optimal configuration of thermotropic glazing was found to provide significant energy savings and improve the comfort of the occupants (Inoue, 2003), including the case of a real building application for retrofitting purposes (Nitz and Hartwig, 2005). Thermotropic glass panes were often tested or simulated when integrated in a simple double-glazing unit (DGU) (e.g. (Yao and Zhu, 2012)), but applications in more complex structures or functions (e.g. a thermotropic glazing that included a heating layer for active dimming control) were also investigated (Inoue et al., 2008).

Dynamic optical and thermophysical properties can also be achieved through the integration of a responsive layer in place of the usual air/gas cavity in multi-pane glazing systems. An example of such an approach is given by the inclusion of a Phase Change Material (PCM) layer (Goia et al., 2014a, 2014b, 2013; S. Li et al., 2016; Silva et al., 2016), whose aim is primarily to improve the exploitation of solar energy through a better control of the direct heat gain.

The concept of PCM glazing is centred around the particular way in which the PCM layer interacts with the impinging solar radiation; it acts as a solar shading device, as a storage medium, and as a moderator of the glazing surface temperature. A PCM glazing system is therefore expected to reduce gains/losses of energy compared to a standard glazing system and to smooth the indoor surface temperature, both in summer and winter. It filters and buffers the incident solar radiation which, during the daytime, may exceed the instantaneous heating demand of the building – shifting the solar gain towards the late afternoon and/or evening, when transmission and ventilation losses are higher. In summer, the PCM layer reduces cooling loads and the indoor surface temperature of the glazing, with a positive impact on both energy demand and comfort conditions. In summary, the introduction of a PCM layer into the glazing system noticeably increases the inertial behaviour of the window.

The first experimental activities related to the integration of PCMs in transparent buildings date back to the late 1990s (Ismail and Henrı, 1998; Manz et al., 1997). Although some intrinsic limitations of the material's properties –

such as low thermal conductivity and volume change during the phase transition (Cuce and Riffat, 2015) – need to be carefully considered, the optical properties of some PCMs (Goia et al., 2015) are promising for integration into glazing systems. They allow the exploitation of the visible part of solar radiation (that is mostly transmitted) for daylight, while a good fraction of the infrared radiation is absorbed by the PCM layer, thus reducing the solar gain in the IR range (Goia et al., 2014b). The effect of thermophysical and optical properties of PCMs in double glazing has also been numerically investigated (D. Li et al., 2016a, 2016b).

1.2 Aims of the research activity

The research activity presented in this paper tests different configurations of responsive glazing systems based on two of the most interesting technologies that enable dynamic optical and thermophysical behaviour of fenestration: PCM layers and thermotropic glass panes. The aim of these advanced fenestration systems is to improve the energy and environmental performance of the transparent envelope through improved management of solar gains. In particular, to overcome some drawbacks that were highlighted in previous research on simple PCM glazing systems (Goia et al., 2014b), the combination of a thermotropic (TT) layer and PCM has been proposed as a possible solution. Two prototypes were tested to collect evidence of the thermophysical behaviour of the proposed system, due to a lack of data in the literature.

In parallel to the two prototypes that integrate PCM with a thermotropic layer, a triple-glazed unit equipped with only the thermotropic layer was tested, so that the influence of PCM and TT combined could be compared against the behaviour of the TT layer alone. Moreover, the experimental campaign investigating the behaviour of the triple-glazed unit with the thermotropic layer alone aims to expand the knowledge of this technology, since the TT layer that was integrated in the prototype had never been tested in a full-scale mock-up.

Finally, a conventional triple-glazed unit with a low-emissivity coating was also tested for reference purposes. In this way, the thermophysical behaviour of the responsive glazing units, as well as their energy and indoor environmental performance, could be compared with that of a well-known technology.

Due to the amount of data that was collected during the experimental campaign, concerning both the thermal and solar optical behaviour of the technologies, for the sake of brevity, this paper only focuses on:

- the description of the prototypes;
- the experimental methods and data processing techniques that were used; and

- the characterisation of the thermophysical properties and the energy performance under winter conditions, in Turin (45.05° N, 7.67° E, Italy), which is a humid subtropical climate (Köppen climate classification Cfa) (Peel et al., 2007).

2 Materials and Technologies

2.1 Materials with dynamic optical and thermophysical properties

2.1.1 Thermotropic glass pane

The thermotropic layer that was adopted in the experimental campaign was a commercially available product, characterised by a switch in optical properties that, according to the technical documentation, takes place in the temperature range of 20 °C to 40 °C. The thermotropic layer was integrated into a laminated glass pane that was made up of a 4-mm thick clear glass pane, a 1.5 mm resin layer (the thermotropic layer), and a 4-mm thick green glass pane, giving a total thickness of approximately 9.5 mm.

The manufacturer's technical datasheet provides the following optical properties, referred to a resin layer of 1.7 mm and a 2×1 mm clear glass: (normal) direct-to-hemispherical solar transmittance 0.69 (low temperature, transparent state) and 0.41 (high temperature, translucent state); visible transmittance 0.69 (low temperature, transparent state) and 0.35 (high temperature, translucent state). The g-value is 0.78 and 0.59, for low temperature and high temperature respectively, with a thermal transmittance of the glass of 5.74 W/(m^2 K).

The optical properties of the actual glass pane used in the experimental activities were characterised by means of a dedicated laboratory investigation (Bianco et al., 2015) that provided the following values: (normal) direct-to-hemispherical solar transmittance 0.45 (low temperature, transparent state) and 0.36 (high temperature, translucent state); visible transmittance 0.66 (low temperature, transparent state) and 0.52 (high temperature, translucent state).

A particular feature of the selected thermotropic glass pane is that the change in the optical transmittance is achieved through an increase in the reflectance of the materials, due to an increase in the difference between the refractive indices of the two main components of the thermotropic layer (Muehling et al., 2009). This last component is made of a polymer layer containing core/shell particles homogeneously dispersed. The particle's core consists of a paraffin wax mixture, whose phase transition is responsible for the change in the ratio of the refractive indices of the core and the shell.

2.1.2 *Phase change material*

The PCM integrated in the prototypes was a commercially available paraffin wax, which was the subject of investigation in a previous study (Goia et al., 2014b). The complete characterisation of the optical properties of this PCM is available in (Goia et al., 2015).

The paraffin wax has a nominal melting temperature of 35 °C and a declared heat storage capacity (in the temperature range 27 °C to 42 °C) of 245 J/g. During both the present and previous experimental activities, the paraffin was found not to be fully compatible with the butyl sealant of the glazing, leading to a degradation of the sealant and to some leakages of the PCM from the glazing cavity. For the future commercial development of the technology, other sealant materials (e.g. silicone-based) should therefore be considered.

The thickness of the PCM layer was 15 mm, the same layer thickness as one of the prototypes that was used in previous studies (Goia et al., 2015, 2014b). For a glazing system comprising two 4 mm (extra clear) glass panes and a 15 mm PCM layer, the resultant (normal) direct-to-hemispherical solar transmittance was 0.46 (solid state) and 0.75 (liquid state), while the visible transmittance was 0.55 (solid state) and 0.85 (liquid state).

Although 15 mm might not be the optimal thickness of a PCM layer within a window system, this value was chosen as a reasonable compromise between a sufficient amount of PCM and the increase in weight of the glazing system. Considering a glazing area of 1 m^2, the increase in weight due to the presence of the PCM, compared to a reference 15 mm air cavity, is approximately 13 kg.

2.2 Materials without dynamic features (clear glass panes)

Thermotropic and PCM layers were integrated in a triple-glazing unit. Three different prototypes were developed and tested at the same time. An 8/15/8/4 mm TGU glazing was used as a reference. The details of its layers are as follows: 8 mm of clear glass pane (τ_e 0.78, ρ_e 0.07 and τ_v 0.88, ρ_v 0.08), 15 mm of cavity with Argon (90%), 8 mm of extra clear glass pane (τ_e 0.89, ρ_e 0.08 and τ_v 0.91, ρ_v 0.08), 15 mm of cavity with Argon (90%), and 4 mm of a low-e glass pane (τ_e 0.66, ρ_e 0.12 front and 0.11 back and τ_v 0.80, ρ_v 0.11 front and 0.10 back, emissivity 0.1). The nominal values of the various layers were adopted to evaluate the thermal transmittance (U), the solar factor (g-value), and the visible and solar transmittance (τ_v and τ_e) of the glazing. For these calculations, WINDOW 7.2 was used.

As far as the other two technologies (TGU_TT+PCM and TGU_TT) are concerned, the same glass panes were adopted and the details of their assemblies are presented in Table 1 and Figure 1.

Table 1 – Features of the tested technologies (from outside to inside).

Layer	**TGU**	*Thickness* [mm]	**TGU_TT**	*Thickness* [mm]	**TGU_TT+PCM(IN)**	*Thickness* [mm]	**TGU_TT+PCM(OUT)**	*Thickness* [mm]
0	-	-	TT glass	9.5	TT glass	9.5	TT glass	9.5
1	Clear glass	8	Clear glass	8	Low-e glass	4	Clear glass	8
2	Argon 90%	15	Argon 90%	15	Argon 90%	15	PCM	15
3	Extra clear glass	8	Extra clear glass	8	Extra clear glass	8	Extra clear glass	8
4	Argon 90%	15	Argon 90%	15	PCM	15	Argon 90%	15
5	Low-e glass	4	Low-e glass	4	Clear glass	8	Low-e glass	4

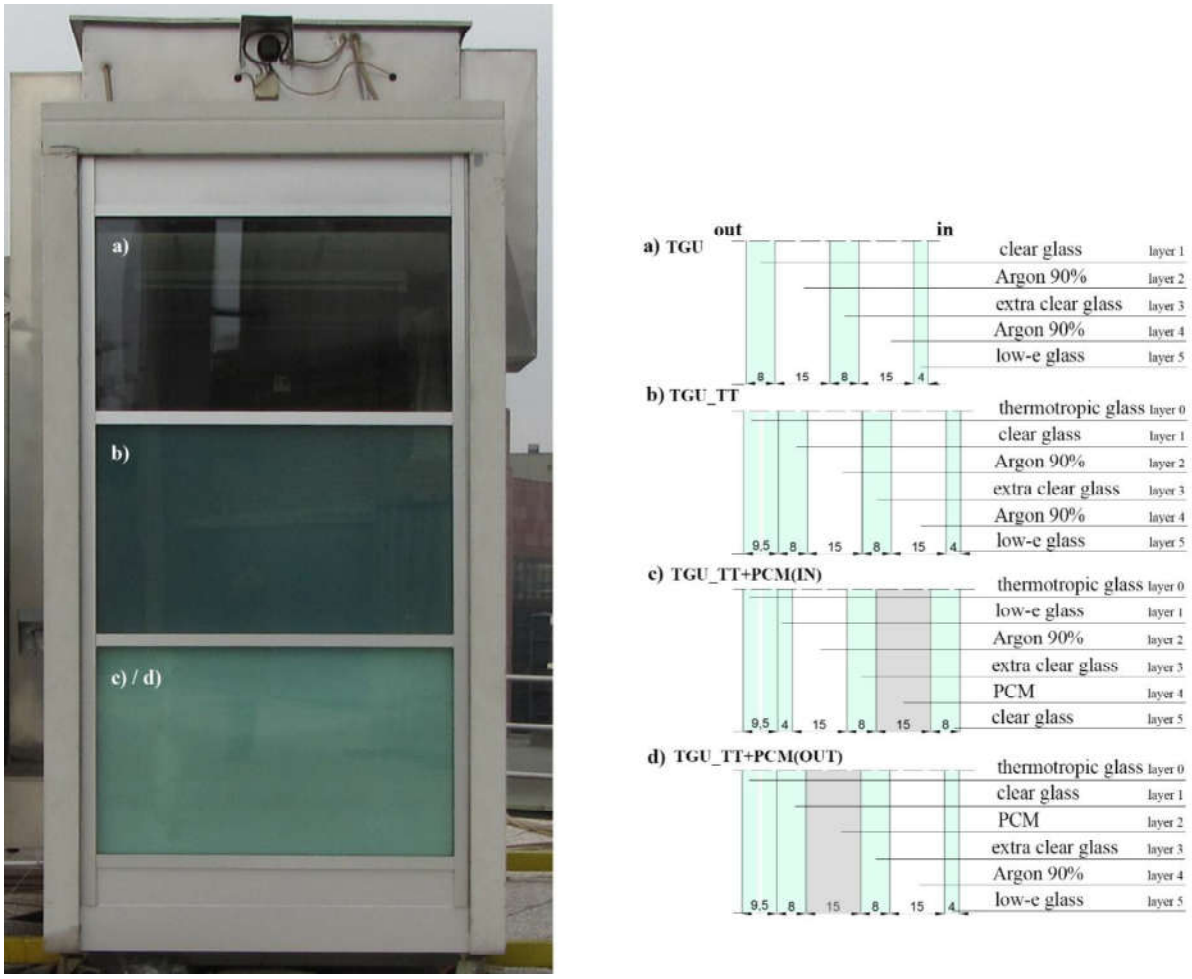

Figure 1 – External view of the test cell (left) and scheme of the tested technologies (right).

2.3 Glazing system prototypes

2.3.1 Triple-glazed unit integrating a thermotropic pane and PCM layer (TGU_TT+PCM)

A previous experimental campaign (Goia et al., 2014b) showed that when the PCM layer is integrated in a double-glazing system, the thermal inertia of the fenestration increases and a reduction of the solar heat gains through the component can be achieved. However, since the thermal resistance of the PCM is lower than that of a gas-filled cavity, the overall thermal resistance of the system is reduced. For this reason, the thermal performance during the heating season (especially during the night or on cloudy days) was found not to be better than that of a traditional component.

As far as thermal comfort was concerned, the PCM glazing was, in general, able to provide a good performance (Goia et al., 2013). However, a negative effect on comfort was observed in summer during the night or when the PCM was completely melted. In such conditions, the indoor surface temperatures of the PCM glazing are higher than those of the reference unit.

To overcome these limits, a new technology was conceived and prototyped (Goia et al., 2014a). This technology is characterised by a triple-glazing unit with a PCM-filled cavity and a thermotropic layer (TGU_PCM+TT).

The switch from a double-glazed unit to a triple-glazed unit was made in order to overcome the drawback of the thermal resistance. The adoption of the TT layer was made to tackle the problems associated with the complete melting of the PCM.

Two configurations of the TGU_TT+PCM technology were tested. The first configuration, named TGU_TT+PCM(IN), presented the PCM-filled cavity towards the indoor environment and the gas-filled cavity towards the outside (Figure 1c), whereas the second configuration, named TGU_TT+PCM(OUT), presented the PCM in the outermost cavity (Figure 1d). The gas-filled cavity was coupled with a low-emissivity coating in one of the two surfaces of the glass panes. The glass panes were a clear and an extra clear pane of 8 mm each, with a 4-mm thick low-e clear glass. The outermost glass pane was always the thermotropic glass described in Section 2.1.1. Details on the construction of the two TGU_TT+PCM can be found in Table 1. The prototypes of the TGU_TT+PCM had a net size of 140 cm width and 80 cm height and a total thickness of 5.95 cm.

The nominal thermal transmittance of the two TGU_TT+PCM prototypes was calculated with the WINDOW 7.2 software. The results are presented in Table 2. A thermal conductivity of the PCM of 0.20 W/(m K) was considered in accordance with the data reported in the technical data sheet, considering only conduction as the heat transfer mechanism within the material.

Table 2 – Nominal thermal transmittance (U), equivalent thermal conductance (C), and equivalent thermal transmittance (U*) of the three tested technologies.*

	U [W/(m^{2}K)]	*C** [W/(m^{2}K)]	*U** [W/(m^{2}K)]
TGU	1.05	1.09	0.92
TGU_TT	1.02	0.93	0.80
TGU_TT+PCM	1.16	1.19	0.99

2.3.2 Triple-glazed unit integrating a thermotropic pane (TGU_TT)

The thermotropic glass pane cannot be used alone in a fenestration system because of the thermal resistance requirements for glazing systems. While the integration of a TT glass pane in a simple DGU might satisfy the

requirements set by some national/local standards, this layer needs to be combined with a triple-glazed structure to achieve a better thermal insulation performance[1].

The schematic representation of the structure of the TGU_TT is shown in Figure 1. The TGU_TT had a net size of 140 cm width, 80 cm height and total thickness of 5.95 cm. The calculated thermal transmittance (WINDOW 7.2) was 1.03 W/(m^2 K) (Table 3). A solar transmittance of 0.22 and 0.18, a g-value of 0.32 and 0.27, and a visible transmittance of 0.37 and 0.30 were obtained with the TT layer in the "off" and "on" states, respectively, as shown in Table 3.

2.3.3 Triple-glazed reference unit (TGU)

The triple-glazed unit, used as the reference case, was a traditional glazing made of two conventional gas-filled cavities and a low-e surface. Details on the construction of the TGU can be found in Table 1 and Figure 1. The net size of the TGU was 140 cm in width, 80 cm height, and a total thickness of 5.0 cm. Optical and thermal properties of the TGU were calculated by means of WINDOW 7.2, starting from the technical datasheet. A nominal solar transmittance of 0.48, a g-value of 0.60, and a visible transmittance of 0.65 were obtained (Table 3).

Table 3 – Measured solar transmittance (τ_e) and visible transmittance (τ_v) of the thermotropic pane, and calculated (WINDOW 7.2) solar transmittance, visible transmittance and g-value of TGU and TGU_TT in "on" and "off" states.

	τ_e	τ_v	*g-value*
Measured data			
TT off (temperature 11 °C)	0.45	0.66	-
TT on (temperature 46 °C)	0.36	0.52	-
Software evaluation			
TGU	0.48	0.65	0.60
TGU_TT off	0.22	0.37	0.32
TGU_TT on	0.18	0.30	0.27

[1] For new buildings, according to the new national Italian law (DM 26/06/2015 transposing EU directive), no specific limits for the thermal transmittance are imposed. The energy performance of the building is compared with that of a reference building. The reference building is designed with a thermal transmittance of the windows (glazing and frame) lower than 1.80 W/(m^2 K) from 2015 for the location of Turin. From 2019, the U value will lower to 1.40 W/(m^2 K) for public buildings only, and from 2021, this requirement will be extended to all other buildings.

2.4 Test rig

The three glazing systems were studied by means of one test cell of the TWINS facility (Serra et al., 2010) (Figures 1, 2). The test cell provides a constant indoor air temperature which, for the winter period, was set to 20 °C. Three samples were installed on the south-exposed façade of the test cell (Figures 1, 2, and 3), so that they were exposed to the same outdoor boundary conditions, while their inside surfaces were in contact with the indoor air, which was kept at a constant, homogeneous, and representative temperature.

Figure 2 – Test cell with sensors: a) external view; and b) internal view.

The experimental campaign lasted, with some breaks, over two years and the two (TGU_TT+PCM) technologies were monitored during the seasons by changing the side (IN/OUT) where the PCM layer was located. The other two technologies (TGU and TGU_TT) were continuously monitored.

Air and surface temperatures, surface heat fluxes, and incident transmitted solar radiation were measured every 5 minutes by approximately 30 sensors connected to a data logger. The measurement chain was verified and calibrated in the laboratory (Figure 3). The monitored data was post-processed in order to obtain average hourly values (temperatures, heat fluxes, and solar irradiance values) or energies transmitted through the glazing.

Surface temperatures were monitored for each technology through TT-type thermocouples installed both on the internal and external surfaces of the glazing prototypes. Indoor surface temperatures of the test cell envelope, indoor and outdoor air temperature, together with temperature of inlet/exhaust air of the full air system of the test cell were also continuously recorded by TT-type thermocouples.

Heat flux meters (Hukseflux HFP01) were located in the centre of the glazing on the internal side. The heat flux meters and temperature sensors directly exposed to solar radiation were shielded from the influence of solar irradiation by means of reflective aluminium foils. It is worth highlighting that, especially in the case of the prototype that integrated both a PCM and TT layer, the presence of the sensors, and of the aluminium foils, may affect the

performance of the glazing system close to the point where physical quantities are measured (see e.g. in (Goia et al., 2014b)). These perturbations are, however, unavoidable in practice.

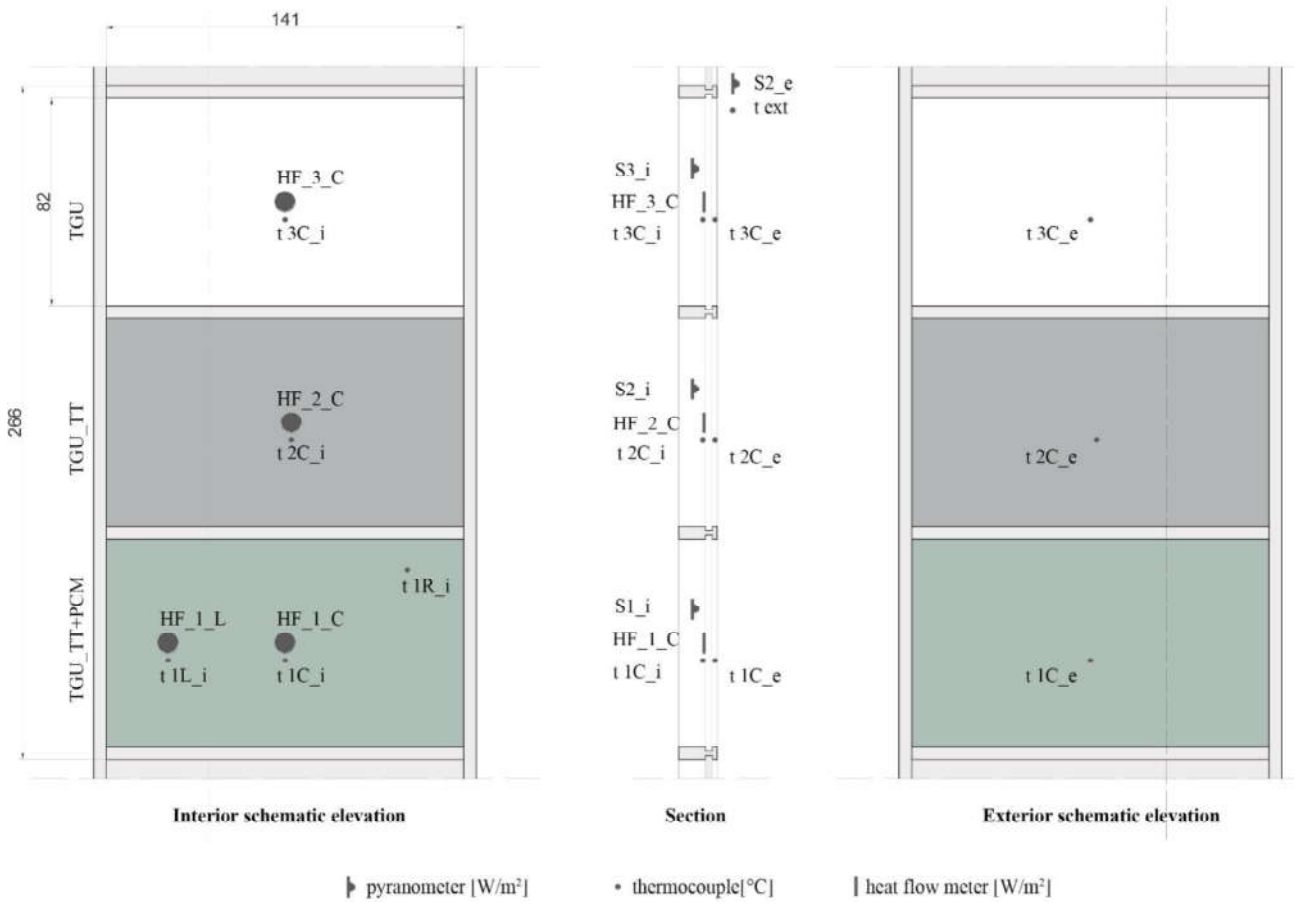

Figure 3 – Schematic view of the test cell with the position of the sensors.

Pyranometers (Hukseflux LP02) were placed behind each technology, parallel to the glazing, to register transmitted solar radiation. An external pyranometer was also installed, parallel to the glazing, to record the impinging solar radiation on the vertical plane.

The resulting accuracies for the entire measurement chain (data acquisition system coupled with sensors) were ±0.5 °C for thermocouples, ±5% for the heat flux meters (leading to an accuracy of approx. ±10% for the daily transmitted energy, see Sections 3.2.2 and 3.2.3) and ±2% for the pyranometers (leading to an accuracy of approx. ±5% for the daily transmitted solar radiation, see Sections 3.2.2 and 3.2.3).

Continuous monitoring was accompanied by spot measurements aimed at assessing the illuminance on the outer and inner surface of the glazing technologies. A MINOLTA lux meter (CL-500A, ±2%, wavelength range 360 nm to 780 nm) was used for these measurements. Measurements were carried out during two significant days, characterised by overcast and clear-sky conditions. During both days, the illuminance was measured from 09.00 to 16.00 with an

hourly time step. Collected data were used to assess the visible transmittance of each glazing (as explained in Section 2.6.1).

The portable lux meter was placed vertically behind each glazing (in the same position as the pyranometers shown in Figure 3) in order to measure the vertical illuminance values transmitted though the tested technologies ($E_{v,in}$). Care was paid to position the sensor close to the glazing; the lux meter was less than 5 cm from the glazing, in order to reduce the influence of the other technologies. Firstly, indoor measurements were performed, moving the sensors behind the three technologies, and secondly, the outdoor vertical illuminance ($E_{v,out}$) in front of the glazing was measured.

Given the architecture of the experimental rig, i.e. a unique indoor environment with the three technologies, all the experimental data was collected at the technologies level, and so direct consideration of the influence of the technologies on the environment was not possible.

2.5 Data selection

One of the major challenges in experimental analyses based on long-term monitoring campaigns is the need to express results by means of comprehensive, yet concise, data or parameters. This means that hourly readings cannot be simply shown all together as an overall; rather, a pre-selection of data is necessary in order to provide useful information. To this end, three types of analysis were carried out after the experiments, focusing on three different timescales:

- data for assessing conventional steady-state parameters (for example, U-value and g-values);
- selection of representative days and selection of representative periods for long-term performance analysis of the dynamic features of the technologies.

2.5.1 Data for conventional steady-state parameters

The first type of analysis includes the determination of the usual thermophysical and optical properties of the glazed technologies alone (e.g. thermal transmittance/resistance, solar heat gain coefficient, visible transmittance). These properties are usually considered to be independent of the boundary conditions although, in practice, they are, to a certain extent, dependent upon them. Their value is, in theory, close to the nominal value typically reported on technical datasheets.

For this type of analysis, large data sets were used in order to cover large periods of time (experimental values collected during the cold season were used) in order to obtain average data that is representative of a large range of boundary conditions. The equivalent thermal conductance (C* [W/(m^2 K)]) and thermal transmittance (U* [W/(m^2 K)])

of the three glazing systems were calculated using this strategy for data selection, according to the procedure described in Section 2.6.1.

2.5.2 Selection of representative days

While analysis of the thermophysical and optical behaviour of conventional glazing technologies might rely on the analysis of steady-state performance parameters alone, an intrinsic complexity is faced when responsive systems are analysed, since they behave differently depending on the boundary conditions. Moreover, an additional problem in the data analysis arises due to the fact that the two prototypes with PCM, namely TGU_TT+PCM(IN) and TGU_TT+PCM(OUT), were tested in different periods of the same season, and hence a direct comparison of their respective performance parameters could not be carried out. All these facts led to the definition of a data selection procedure based on the definition of representative days, as already previously adopted in similar analyses of responsive glazing systems (Goia et al., 2014b, 2013). This procedure is designed to analyse the dynamic performance of the envelope components under different, extreme, boundary conditions, enabling a comparison of the technologies.

To select appropriate days and to assess their representativeness, a double frequency distribution analysis of the monitored daily mean external temperature and global vertical irradiation was performed over the whole duration of the experimental campaign. In Figure 4, this frequency analysis is plotted as a colour coded area: the darker the area on the graph, the higher the number of days characterised by analogous daily mean external air temperature and global vertical irradiation.

Four representative days were finally selected out of the entire set of data correspondent to the winter season:

- Two similar days (Day 1 and Day 2) characterised by low daily irradiation (H [kWh/m^2]) on the vertical plane and low outdoor air temperature (ϑ [°C]) (i.e. bad weather days):
    - Day 1, when the TGU_TT+PCM(IN) was tested;
    - Day 2, when the TGU_TT+PCM(OUT) was tested.
- Two similar days (Day 3 and Day 4) characterised by high daily irradiation (H [kWh/m^2]) on the vertical plane and low outdoor air temperature (ϑ [°C]) (i.e. sunny but cold days):
    - Day 3, when the TGU_TT+PCM(IN) was tested;
    - Day 4, when the TGU_TT+PCM(OUT) was tested.

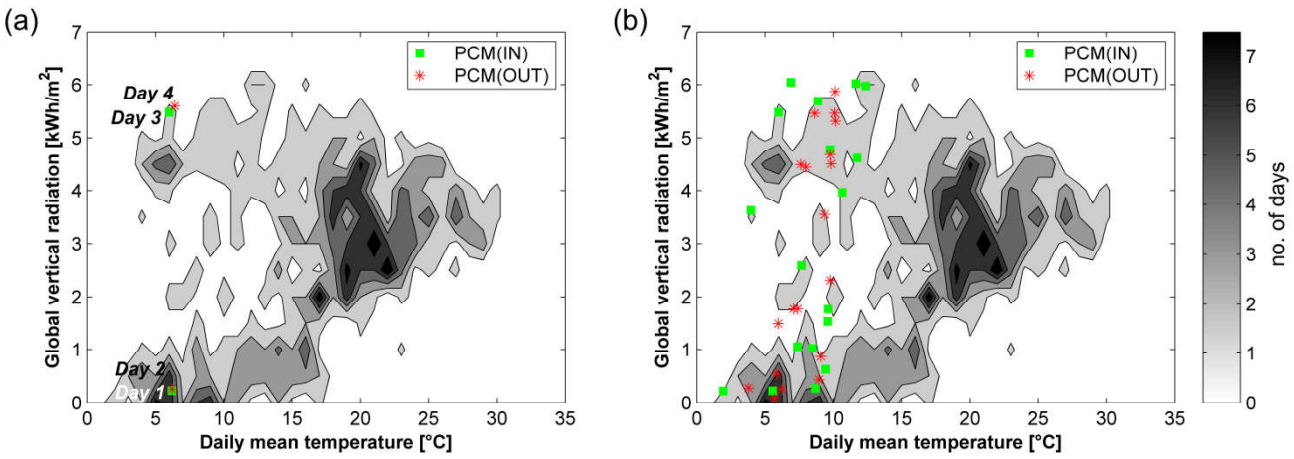

Figure 4 – Frequency distribution of the weather data expressed as the number of days having the same combination of global vertical irradiation and daily mean temperature: (a) days selected for daily analysis; and (b) days selected for the long-term performance evaluation.

The boundary conditions of these representative days are plotted in Figure 5. It can be seen that each couple of days (Day 1 and Day 2; Day 3 and Day 4) is characterised by similar boundary conditions, such that a comparison between the two TGU_TT+PCM configurations can be considered accurate and reliable. In Table 4, the daily values of solar irradiation (H), average external temperature ($\vartheta_{air,out,average}$) and temperature excursion (ϑ_{ex}) are shown for the four representative days. The temperature excursion was calculated as the difference between the maximum and the minimum daily value of the outdoor air temperature.

The representative days were used to compare the time profile of the heat flux exchanged at the indoor surface of the glazing systems, the transmitted solar irradiance, and the visible and solar transmittance. Furthermore, the daily energy crossing the glazing system was also assessed for every technology during the representative days (as explained in Section 3.2.3).

Table 4 – Boundary conditions of the selected days: solar irradiation, average external air temperature, and external air temperature excursion.

		H	$\vartheta_{air,out,average}$	ϑ_{ex}
		[kWh/m^2]	[°C]	[°C]
TGU_TT+PCM(IN)	*Day 1 cold+cloudy*	*0.23*	*5.4*	*2.9*
TGU_TT+PCM(OUT)	*Day 2 cold+cloudy*	*0.25*	*5.1*	*5.0*
TGU_TT+PCM(IN)	*Day 3 cold+sunny*	*5.38*	*6.0*	*8.6*
TGU_TT+PCM(OUT)	*Day 4 cold+sunny*	*5.59*	*7.1*	*13*

2.5.3 Selection of representative periods for long-term energy performance analysis

The long-term performance analyses complemented the analyses on the representative days and were aimed at giving a synthetic evaluation of the total energy performance of the systems over a longer period of time, which may be

considered representative of the winter season. Two sets of 18 consecutive days were selected, Set 1 for TGU_TT+PCM(IN) and Set 2 for TGU_TT+PCM(OUT), using the double frequency distribution analysis previously presented. In Figure 4b, the two sets of data (consisting of 18 days each) are plotted. It can be seen that, in each set, both cold cloudy and sunny days were included, as well as different outdoor air conditions. In parallel to a qualitative comparison of the two periods, a quantitative evaluation was carried out through the calculation of the heating degree day (HDD) for each set (as described in Section 2.6.3), applying Equation 5. This led to the following HDD values: 226 °C day and 212 °C day, respectively for Set 1 and Set 2.

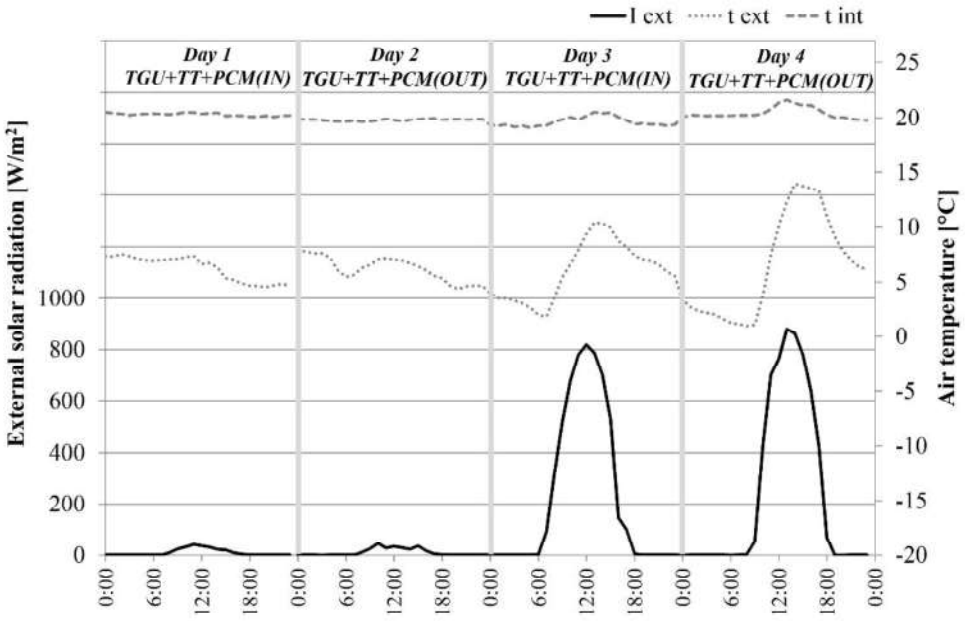

Figure 5 – Boundary conditions of the selected days; hourly time profiles of external solar radiation and air temperature.

2.6 Performance parameters adopted for the data processing and analysis of the glazings

2.6.1 Conventional steady-state parameters

- The equivalent thermal conductance (C^* [W/(m^2 K)]) of the three systems was assessed through the linear regression of the surface heat fluxes and the temperature difference between outer and inner surfaces.

  To avoid the disturbances due to the solar radiation and to reduce the impact of the dynamic effects of the components, only night values between 02:00 and 06:00 were used to evaluate the equivalent thermal conductance. In addition, in order to improve the accuracy, only data with an air temperature difference between indoor and outdoor greater or equal to 10 °C was used. As a result, the equivalent thermal conductance was evaluated using a set of 235 data values (that is, pairs of indoor surface heat flux vs. temperature difference values).

- The equivalent thermal transmittance (U^*) for the three technologies was obtained by adding the nominal internal and external surface resistances to the equivalent thermal conductance (C^*), as suggested by EN ISO 6946:2007 (EN, 2007) (0.17 m^2 K/W and 0.04 m^2 K/W, respectively).

2.6.2 Hourly profiles and total daily energy

The hourly profiles of the following physical properties were analysed for the representative days in order to obtain an in-depth understanding of the dynamic behaviour of the three glazing systems.

- The outdoor surface temperature, $\vartheta_{surf,out}$ [°C]; this quantity gives information on the state (on/off) of the thermotropic layer.
- The heat flux, $\dot{q}_{surf}$ [W/m^2], exchanged at the indoor surface of the glazing system (including the heat exchanged by convection with the indoor air and by radiation in the long-wave IR region with the other surfaces of the test cell).
- The transmitted solar irradiance, I_{in} [W/m^2]; measured by the pyranometers installed at the rear of the glazing samples.
- The solar transmittance, τ_e [-]; assessed as the ratio of solar irradiance measured by the internal vertical pyranometer, I_{in} [W/m^2], to the solar irradiance measured by the external pyranometer, I_{out} [W/m^2]:

$$\tau_e = \frac{I_{in}}{I_{out}} [-] \quad (1)$$

- The visible transmittance, τ_v [-];assessed as the ratio of the illuminance measured on the vertical plane at the rear of the glazing system, $E_{v,in}$ [lx], to the illuminance measured on the outdoor vertical plane, $E_{v,out}$ [lx]:

$$\tau_v = \frac{E_{v,in}}{E_{v,out}} [-] \quad (2)$$

- The total daily energy, $E_{24,tot}$ [Wh/m^2]; calculated as the integral over 24 hours of the total heat flux, $\dot{q}_{tot}$ [W/m^2], crossing the glazing system. This quantity is the sum of the indoor surface heat flux, $\dot{q}_{surf}$ [W/m^2], measured with the heat flux meters, and of the transmitted solar irradiance, I_{in} [W/m^2], measured with the pyranometer:

$$\dot{q}_{tot} = \dot{q}_{surf} + I_{in} [\mathrm{W/m^2}] \quad (3)$$

The integration limits for the calculation of the total daily energy, $E_{24,tot}$ [Wh/m^2], were chosen from 07:00 to 07:00 + 1 day, in order to exclude the effect of the solar irradiation of the previous day on the analysis of the present day:[2]

$$E_{24,tot} = \int_{t=07:00}^{07:00\ +1day} \dot{q}_{tot}\, dt \quad (4)$$

2.6.3 Long-term total energy

The analysis of the seasonal performance of the glazing systems was performed through the total energy parameter, which is an extension of the daily total energy concept. A normalisation over heating degree days was performed in order to reduce, as much as possible, the influence on the results of slightly different boundary conditions of the two sets of data (Set 1 and Set 2) chosen for the two different technologies that integrate the PCM and the TT layers.

The normalised total energy, $E_{n,tot}$[Wh/(m^2 °C)], was evaluated as the summation of the 18 consecutive daily total energy values, $E_{24,tot}$ [Wh/m^2], normalised over the HDD value of the same days:

$$HDD = \sum_{n=1}^{18\ day}(\bar{\vartheta}_{in} - \vartheta_{out})\ [°C{\cdot}day] \quad (5)$$

$$E_{n,tot} = \frac{\sum_{n=1}^{18\ day}(E_{24,tot})}{HDD}\ [Wh/(m^2\ °C)] \quad (6)$$

3 Results and Discussion

3.1 Steady-state thermophysical parameters

The results of the equivalent conductance (C* value) analyses are shown in Figure 6. The introduction of the PCM inside one of the two cavities did not significantly decrease the thermal resistance of the system, as expected (thanks to the second gas cavity). However, it must be mentioned that the overall conductance was slightly increased, even considering that the TGU_TT+PCM glazing had, in practice, an additional 9 mm glass layer. The resistance due to this layer can be estimated to be 0.16 m^2 K/W. The reference technology (TGU) presented a thermal conductance of 1.09 W/(m^2 K), whereas a higher value of 1.19 W/(m^2 K) was found in the case of TGU_TT+PCM(OUT). The same value was calculated for the configuration with the PCM in the inner cavity (IN). This confirmed that the new TGU_TT+PCM concept enabled the goal of a high thermal resistance to be realised.

A slightly lower *C** value, 0.93 W/(m^2 K), was calculated for the TGU_TT.

The coefficient of correlation evaluated for TGU_TT+PCM ($R^2 = 0.85$) was the lowest among the three technologies. This is probably due to the strongly dynamic behaviour of the prototype and to the increased thermal inertia of the component (even in the coldest part of the night, the element did not behave as a purely resistive assembly

[2] The PCM layer, in those technologies that make use of it, accumulates thermal energy, converting it from the absorbed solar radiation. During the night, the PCM solidifies, releasing this energy. It has been verified that the discharge phase of the PCM was always finished by 07:30.

– the other two glazing systems did). The calculated *C** value for TGU_TT+PCM is representative of the PCM in solid state, since the evaluation was conducted with winter and night data only.

The corresponding equivalent thermal transmittances, shown in Table 2, are: 0.92 W/(m^2 K) for TGU, 0.80 W/(m^2 K) for TGU_TT, and 0.99 W/(m^2 K) for TGU_TT+PCM. The thermal transmittance (*U* values) evaluated with the software were slightly higher than the values calculated from experimental data (*U** values) for all the three technologies. This is probably due to a different surface resistance both at the indoor and outdoor surfaces of the glazing system. However, the experimental data is in good agreement with the calculated data, and the trend shown by the simulated values (the most-insulated, mid-insulated and worst-insulated glazing systems) is confirmed by the experimental analysis.

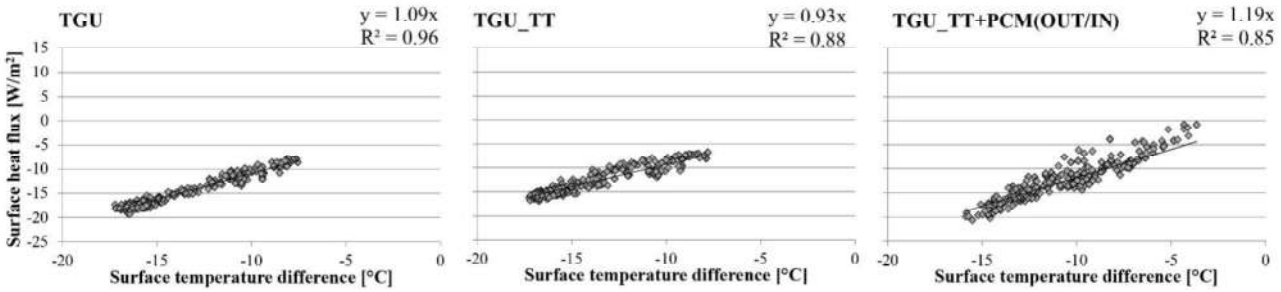

Figure 6 – Equivalent thermal conductance (C) for TGU (a), TGU_TT (b) and TGU_TT+PCM(OUT/IN) (c).*

3.2 Daily analyses

3.2.1 Optical properties

As far as the assessment of the solar and optical behaviour is concerned, the hourly values of illuminance and solar radiation measured on the façade and transmitted through the glazing systems from 09:00 to 16:00 on the two selected days (clear sky and cloudy day) are shown in Figure 7a and 7b and Figure 8a and 8b, respectively.

These profiles were used to assess the solar and visible transmittance (calculated respectively with Equations 1 and 2) of the three glazing technologies (i.e. TGU, TGU_TT, TGU_TT+PCM). The resulting hourly profiles during a cloudy and a sunny winter day are shown in Figure 7 and Figure 8c and 8d. During the cloudy day (0.36 kWh/m^2 of solar irradiation), the thermotropic glazing was in the "off" state and the PCM remained solid throughout the whole day. The visible transmittance (Figure 7c) of the TGU_TT ranged between 28% and 40%, whereas the visible transmittance of the reference TGU ranged between 49% and 69%. Although the thermotropic layer was in the "off" state (due to the low temperature), the visible transmittance was almost halved compared to the TGU. The visible transmittance of the TGU_TT+PCM was very stable at a value of around 3%.

During the sunny day (5.83 kWh/m^2 of solar irradiation), the visible transmittance (Figure 7d) of the reference TGU was approximately 70%. The thermotropic layer entered the "on" state at 13:30/14:00 and the visible transmittance of the TGU_TT during the afternoon was about 25%. The visible transmittance was more than halved when compared to the reference, although not such a big difference was measured between the "on" and "off" states of the thermotropic layer. The visible transmittance of the TGU_TT+PCM during the morning hours, when the PCM was solid, was about 2%. By 14:00, the PCM had undergone complete melting, and the visible transmittance had risen to approximately that of the TGU_TT.

The solar transmittance (τ_e) of the reference technology (TGU) was approximately 40%, whereas a solar transmittance value of approximately 17% was found for the TGU_TT (Figure 8c and 8d). Concerning the TGU_TT+PCM, the solar transmittance was always below 5% during cloudy days, with the PCM in either the inner or the outer cavity, with values ranging between 1% and 3% (Figure 8c). During the sunny day, the PCM melted at around 14:00. The solar transmittance of the TGU_TT+PCM was the same as that of the TGU_TT (Figure 8d), as it was for the visible transmittance (τ_v).

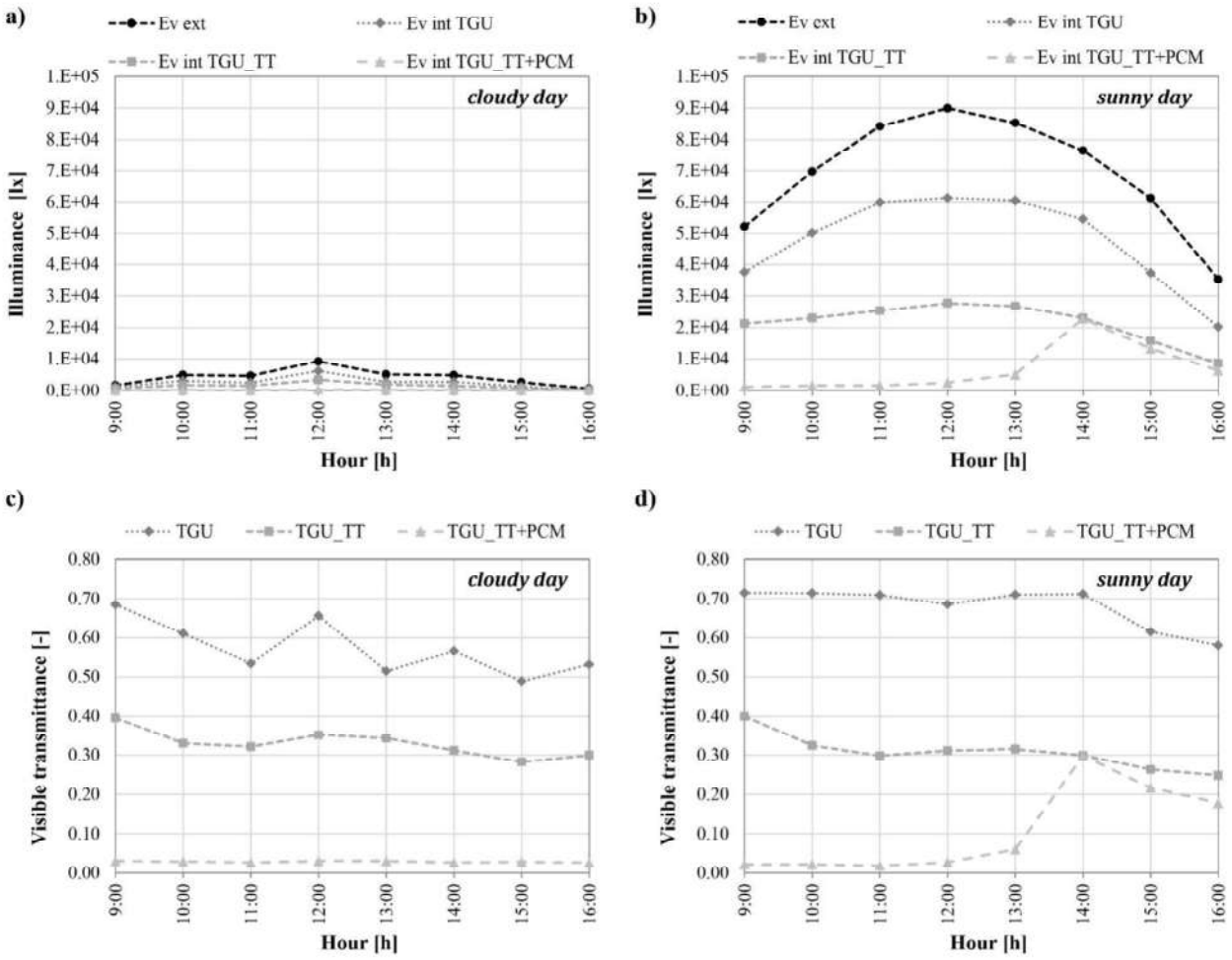

Figure 7 – Measured vertical illuminance values: a) cloudy day; b) sunny day. Visible transmittance: c) cloudy day; d) sunny day.

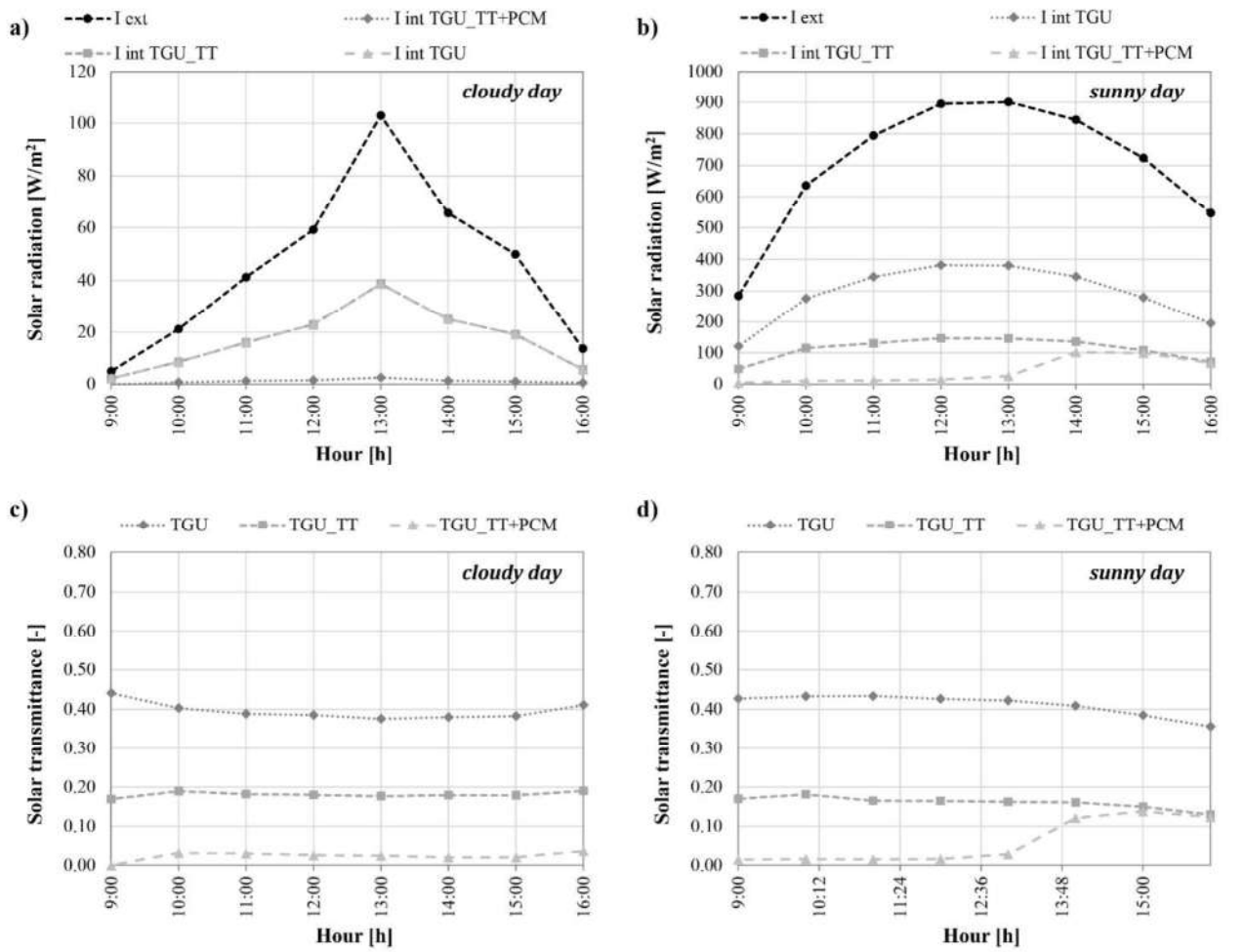

Figure 8 – Measured vertical solar irradiance values: a) cloudy day; b) sunny day. Solar transmittance: c) cloudy day; d) sunny day.

3.2.2 Thermophysical behaviour and daily transmitted energy during cloudy days

The time profiles of surface heat fluxes, transmitted solar radiation, and total heat fluxes (calculated with Equation 3) during cloudy heating-season days (Day 1, PCM(IN) and Day 2, PCM(OUT)) are plotted in Figure 9. During those days, the surface heat fluxes through the three technologies were similar. During the whole of Day 1, the surface heat fluxes through TGU_TT+PCM(IN) were negative (i.e. exiting from the room), with values of approximately -14 to -9 W/m^2 and the same behaviour was found for TGU_TT+PCM(OUT) during Day 2. Outdoor surface temperatures of the three technologies showed a similar trend as that shown in Figure 9b; the measured values were between 10 °C and 4 °C, corresponding to the "off" state of the thermotropic layer. Since the solar radiation was very low, no significant difference was observed when varying the PCM position (inner and outer cavity) as the PCM remained in solid state during both days. Nevertheless, as shown by the temperature trend in Figure 9b, when the PCM is located in the inner

cavity, the thermal inertia of the system increases slightly; the surface outdoor temperature is slightly lagging that of the TGU and TGU_TT technologies. This is, however, a small effect that does not have any practical implication.

A positive total heat flux was only achieved by the reference technology (TGU), meaning that the solar properties of the other two technologies (TGU_TT and TGU_TT+PCM) did not allow for the exploitation of any free solar gain when the sky was cloudy. However, the heat fluxes during the night were quite similar (around -13 W/m^2) for all the technologies. Hence, the integration of the PCM into a triple-glazing system did not lead to significantly higher heat losses compared to the TGU. A deeper and more refined analysis of Figure 9a reveals that from a mostly theoretical point of view, the presence of the PCM gives rise to a small increase in the exiting surface heat fluxes, in particular during the night-time. This is indeed in good agreement with the results of Section 3.1, where the U value of the TGU_TT+PCM glazing (Table 2) turned out to be slightly higher than that of the TGU and TGU_TT components. The comparison between the behaviour of the TGU_TT+PCM(IN) and of the TGU_TT+PCM(OUT) (Figure 9a) shows that the latter has a marginally worse behaviour, with exiting surface heat fluxes that are 1–2 W/m^2 higher. Nevertheless, as already highlighted for the outdoor surface temperatures, all those differences have almost no practical relevance as far as the energy performance of the technologies is concerned; they do, however, indicate that the reliability of the obtained results is satisfactory (that is, the measured static parameters do reflect the monitored physical behaviour of the component).

These findings are confirmed by the assessment of the daily total energy exchanged through the glazing ($E_{24,tot}$, calculated with Equation 4, Figure 10). A value of -288 Wh/m^2 was calculated for TGU_TT+PCM(IN) and -309 Wh/m^2 for TGU_TT+PCM(OUT).

For the reference technology (TGU), -166 Wh/m^2 and -171 Wh/m^2 were respectively calculated during Day 1 and Day 2. No relevant difference in terms of performance of the TGU_TT could be observed for Day 1 and Day 2 due to the fact that the thermotropic was, in both days, far from the transition phase; an energy loss of -215/-219 Wh/m^2 was calculated. It is worth mentioning that the difference in the daily total energy between the TGU and the TGU_TT is only 4–5 Wh/m^{2}day switching from Day 1 to Day 2; a negligible value, being lower than the measurement accuracy. When comparing the TGU_TT+PCM(IN) and TGU_TT+PCM(OUT) components, the difference rises to 21 Wh/m^{2}day; still a very small value, but detectable. Such a result is consistent with the fact that, most probably, when the PCM is located on the outside part of the glazing, the (small) energy accumulated in the layer during the day (as sensible heat in this case, since the PCM does not melt) is, for the most part, exchanged with the outdoor environment. On the contrary, when the PCM is located inside, the additional thermal resistance of the gas cavity allows for better exploitation of the buffered energy (which is released towards the room).

According to the disaggregated analysis of the entering/exiting daily energies (shown in Figure 11), the negative energy loss is not counterbalanced by the positive solar gains during cloudy and cold days. To summarise, during cloudy days the energy loss from the TGU_TT+PCM was 42–45% higher compared to the reference TGU, and 24–30% higher compared to the TGU_TT, regardless of the PCM's position. The dynamic behaviour of the TGU_TT and TGU_TT+PCM glazings cannot be properly exploited.

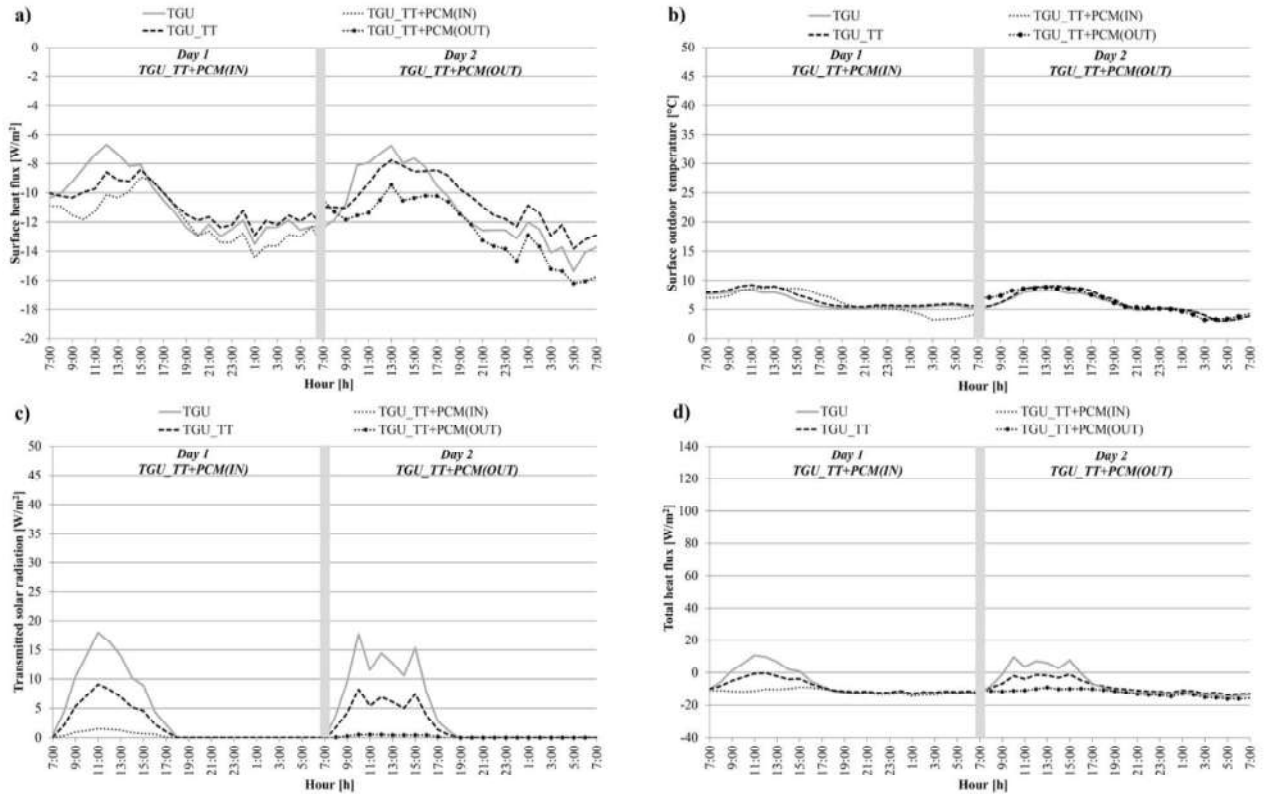

Figure 9 – Day 1 and Day 2 (cloudy day): a) surface heat flux, b) outdoor surface temperature, c) transmitted solar radiation, and d) total heat flux.

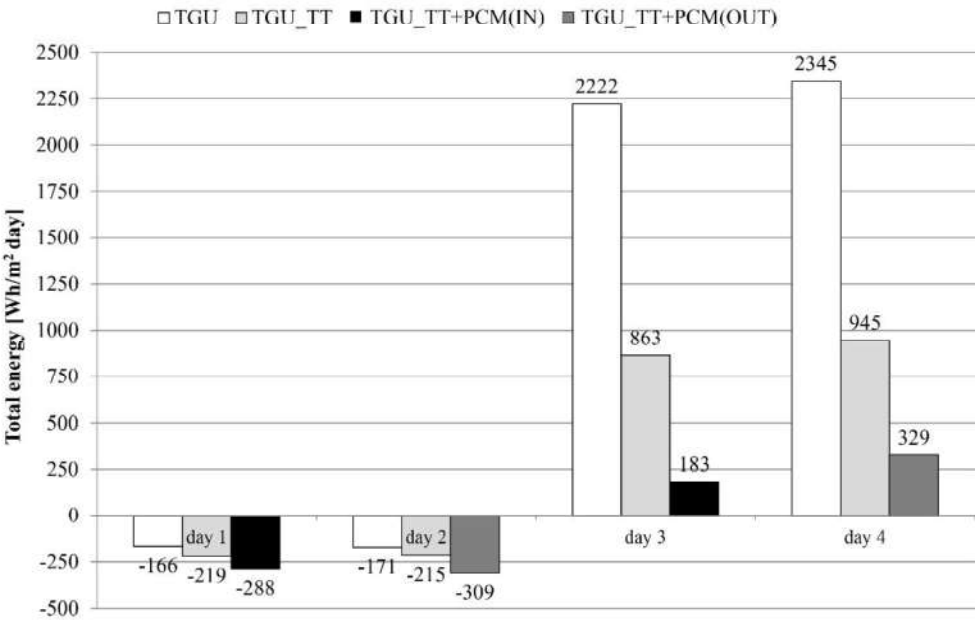

Figure 10 – Daily total energy crossing the technologies.

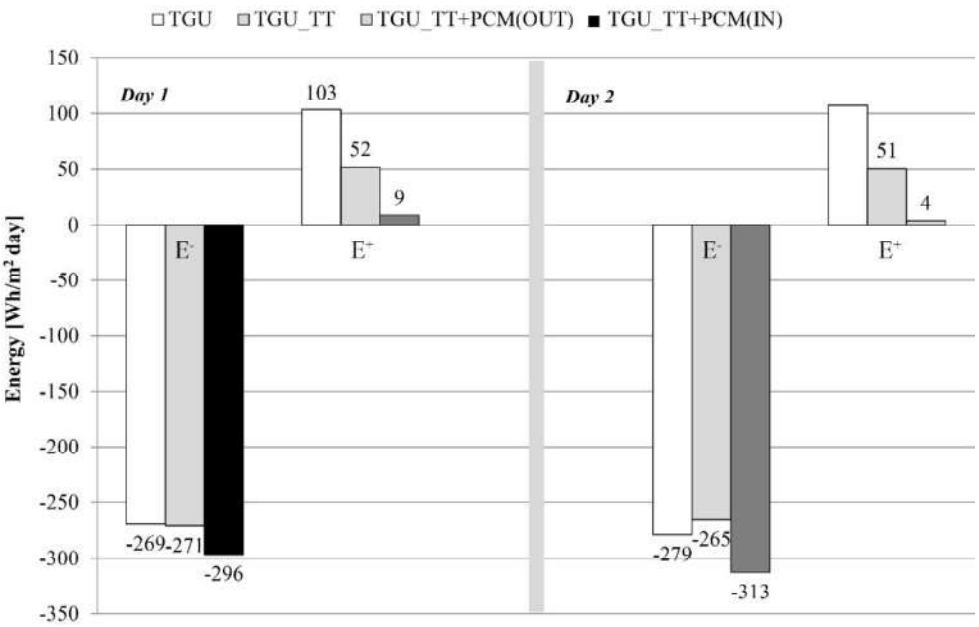

Figure 11 – Daily energy crossing the technologies. E^- are the energy losses (negative) and E^+ are the energy gains (positive).

3.2.3 Thermophysical behaviour and daily transmitted energy during sunny days

During sunny days (Day 3, PCM(IN) and Day 4, PCM(OUT)), the position of the PCM had a significant influence on the performance of the technologies, as can be seen in Figure 12.

During Day 3, TGU_TT and TGU_TT+PCM(IN) had a similar pattern of surface heat fluxes, with a peak value of nearly 40 W/m^2 for both technologies. However, a two-hour shift can be observed for the TGU_TT+PCM(IN), due to the higher thermal inertia of this glazing (13 kg of PCM are introduced in the cavity). It is, however, worth noting that the phase transition of the PCM did not occur during Day 3. This fact is confirmed by the transmitted solar radiation; as no values greater than 20 W/m^2 were detected (Figure 12c). On the contrary, during Day 4, the phase transition of the PCM in the TGU_TT+PCM(OUT) did take place, having a remarkable impact on the surface temperature of the glazing, the transmitted solar irradiance, and the total energy crossing the glazing system during the 24 hours (Figure 12b). During Day 3 (Figure 12 b), the outdoor surface temperatures of TGU_TT and TGU_TT+PCM(IN) had a similar trend but higher values than the reference TGU technology. This can be explained by the fact that the coefficient of absorptivity of the technologies with the thermotropic layer was higher than that of the TGU. Contrastingly, during Day 4, TGU_TT+PCM(OUT) showed a different trend of the surface outdoor temperature, confirming that the phase transition of the PCM was taking place. From 14:00 onwards, the PCM was in liquid state and

the transmitted solar radiation quickly increased from 20 W/m^2 to 60 W/m^2 (Figure 12c). At least half of the mass of the PCM was in liquid state and fully transparent.

In terms of global thermal performance, the melting process, and the consequent exploitation of the latent heat of the PCM, led to a reduction of the peak heat fluxes when compared to the reference technology and the TGU_TT. Starting from 16:00 of Day 4, TGU and TGU_TT presented decreasing surface heat fluxes, whereas TGU_TT+PCM(OUT) presented a stable value of about 20 W/m^2 (Figure 12a). This can be explained by the discharging phase of the PCM. The surface heat fluxes through the TGU_TT presented a similar trend to the solid state of TGU_TT+PCM(IN). Comparing the thermotropic technology (TGU_TT) with the reference one (TGU), a 38–39% reduction of the peak transmitted solar radiation can be observed (Figure 12c). As expected, the lowest transmitted solar energy was registered for the PCM-filled technologies. The effect of the PCM on the transmitted solar radiation can be inferred by comparing TGU_TT+PCM with TGU_TT technology. During Day 3, the peak reduction in terms of transmitted solar radiation was about 83%. The same reduction occurred during the first hours of Day 4, when the PCM was still solid. Once the PCM was in liquid state (after 14:00), the difference was reduced to 31%. The same considerations apply also for the total transmitted solar radiation.

These features highlight some interesting considerations about the comparison of the various glazing schemes and the desired performance in terms of energy efficiency. Firstly, as far as the two PCM technologies are concerned, it is clear that the location of the PCM layer towards the indoor side (TGU_TT+PCM(IN)) implies a lower exploitation of the incident solar radiation. The melting process does not happen, even during sunny days. Only a small increase in thermal inertia is obtained in comparison with the TGU_TT glass. (The sensible heat accumulation in the 13 kg of PCM translates into a temperature–time profile delay of about 2 hours, see Figure 12a.) On the contrary, when the PCM is located in the outermost cavity (TGU_TT+PCM(OUT), it is possible to collect and store a larger amount of solar energy in the glazing. The coupling of the TT (characterised by a considerable absorption of the solar radiation) and the PCM enables the transition temperature to be reached and, hence, the exploitation of the latent heat of fusion (as can be observed by looking at the profiles of the transmitted solar energy and surface/total heat fluxes after 14:00 in Figure 12a and 12c).

While a reduction in the direct solar gain may be seen as a less-preferable behaviour compared to other more "transparent" glazing systems, it is important to highlight how in the framework of highly insulated buildings with relatively large glazed surface, direct solar gain in winter time can lead to an overheating risk. This means that the reduction in the transmitted solar radiation, especially during the central hours of the day (i.e. 10:00 to 15:00), may be beneficial in many situations.

For example, looking at Figure 12d, and imagining to adopt either the TGU, or the TGU_TT or, finally, the TGU_TT+PCM glazing in a hypothetical building, the chances are that in the case of the TGU, the environment will overheat from between 10:00 and 16:00–18:00 due to a significant peak in the entering total heat flux (transmitted short-wave plus surface). Afterwards, the space shows a considerable heating energy demand since the heat fluxes suddenly become negative (i.e. heat losses). The TGU_TT and TGU_TT+PCM(IN) technologies are indeed able to prevent the overheating (peak values of about 150 W/m^2 compared to the 360–370 W/m^2 of the TGU), but will present the same behaviour and drawbacks of the TGU for the time period from 16:00–18:00 onwards. In contrast, the TGU_TT+PCM(OUT) is able to keep the solar loads to a reasonable level (around 75 W/m^2) by storing a large amount of heat at an almost constant temperature, thereby preventing the risk of overheating of the rooms. In addition, this stored energy can be released at a later time (after 17:00–18:00) when the heating demand of the building is higher. Such behaviour allows for better exploitation of the solar energy, because it is possible to accumulate and redistribute the free gains, thus augmenting their so-called utilisation factor.

These conclusions are also supported by the analysis of the energy crossing the glazing during Day 3 and Day 4 (shown in Figure 10). The total energy through the TGU was 2222 Wh/m^2 and 2345 Wh/m^2 during Day 3 and Day 4, respectively. A 60% reduction was obtained with the TGU_TT, and a further decrease was found for the TGU_TT+PCM technologies. When compared against the reference TGU, a reduction of the total energy crossing the glazing along the 24 hours of 92% and 86% were obtained for the TGU_TT+PCM(IN) and TGU_TT+PCM(OUT), respectively. From Figure 10, it is clear that the peculiar behaviour of the technologies with PCM (both in the inner and outer cavity) was mainly due to the reduction of the solar gains.

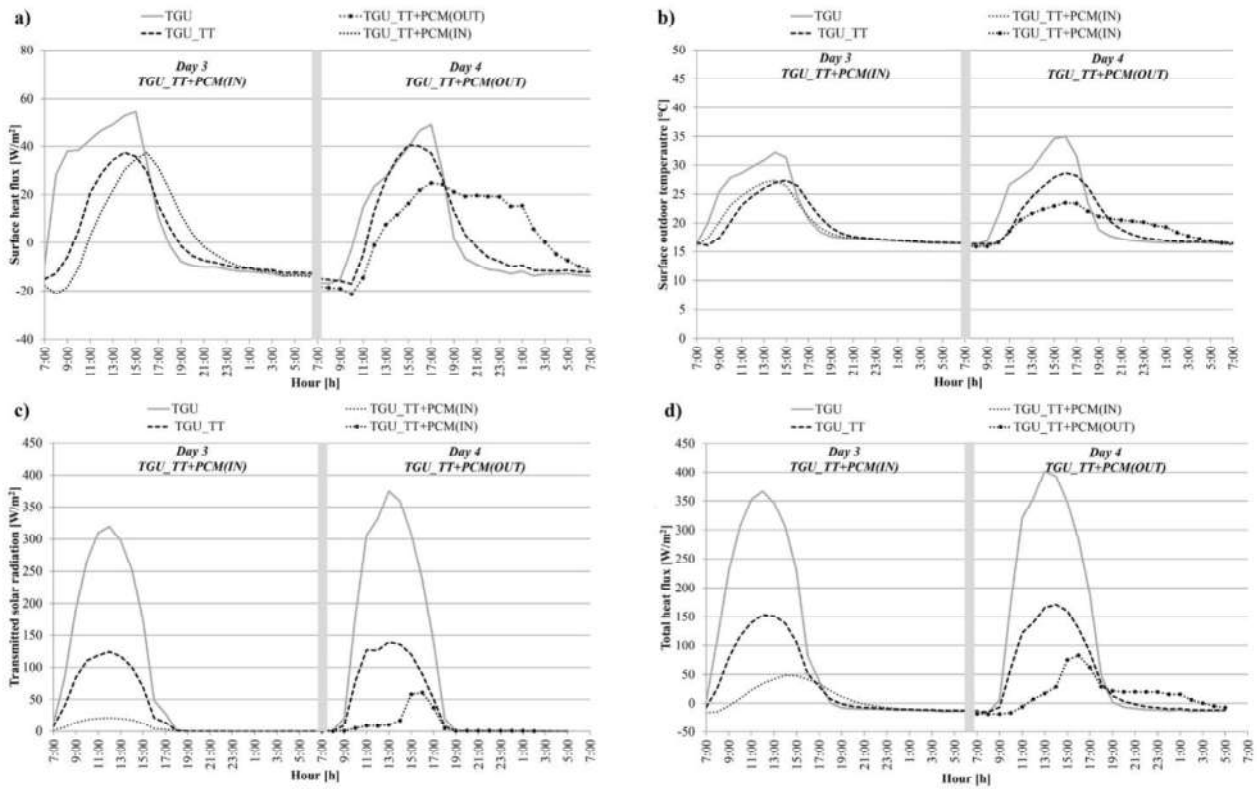

Figure 12 – Day 3 and Day 4 (sunny days): a) surface heat flux, b) outdoor surface temperature, c) transmitted solar radiation, and d) total surface heat flux.

3.3 Long-term energy performance

The results of the long-term performance evaluation are presented in Figure 13, where the total normalised energy (*En,tot,* calculated with Equation 6) crossing the glazing systems over the entire period (18 days) is shown. The normalised energy through the TGU and the TGU_TT, calculated for the first dataset, was very similar to the corresponding values calculated for the second data set, indicating the good comparability of the two datasets.

As far as the TGU_TT+PCM technology is concerned, the net energy (the algebraic sum of energy entering and leaving the indoor environment) was almost zero. Although reduced, the solar gains were still almost capable of balancing the heat losses. A contrasting performance between the two PCM configurations was observed. When the PCM layer was in the outermost position, TT+PCM(OUT), the normalised energy through the technology was very small but positive, whereas it was slightly negative when the PCM was placed in the inner cavity. This behaviour is in line with the results from the daily analyses for the sunny days. The latent heat of the PCM could only be exploited when the PCM was placed in the outer cavity, with the following two impacts on the performance of the technology. Firstly, the solar heat gains became slightly higher when the PCM was liquid due to the increased solar transmittance of the component. Secondly, the heat losses were reduced when the stored latent heat was discharged during the night. However, it must be considered that the difference, in terms of total energy between the two positions of the PCM-filled cavity during the heating season, is very small and similar to the uncertainty of the experimental analysis.

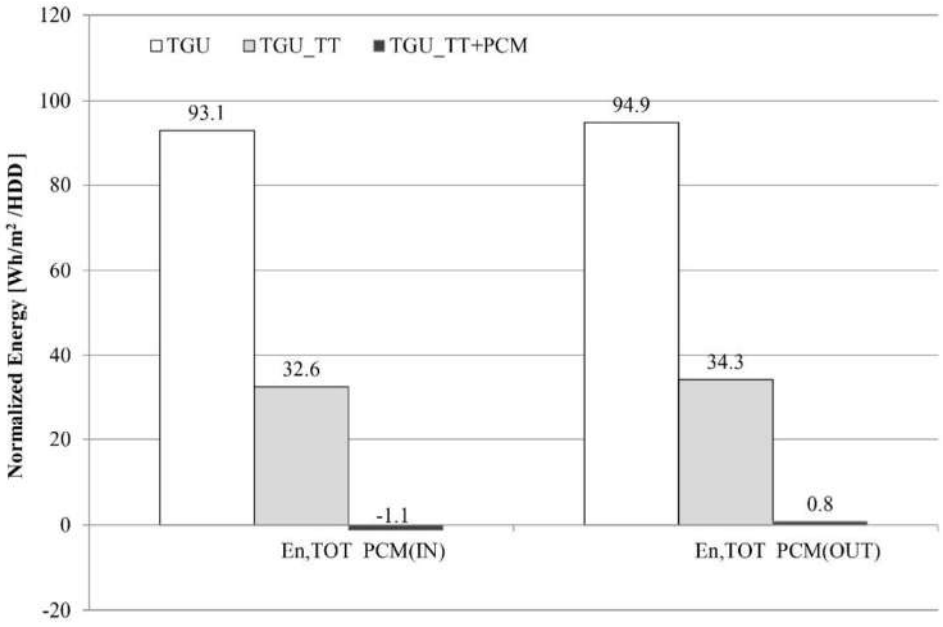

Figure 13 – Normalised total energy crossing the technologies, over a period of 18 days.

3.4 Considerations on thermal comfort

Energy performance analyses in buildings must also go alongside the evaluation of the indoor environmental quality. A thermal comfort analysis, based on the evaluation of the PMV and PMV* indices was therefore carried out for the winter season for the three glazing systems, using data from the representative days. However, for the sake of brevity, no detailed description of this analysis, which was conducted according to the international standard EN ISO 7730:2005 (EN, 2005), is given in this paper.

The three glazing systems tested presented a good thermal resistance, meaning that their indoor surface temperature was always high enough to ensure conditions of thermal comfort. When dealing with glazing systems, the most-likely source of local discomfort is an excessive radiant temperature asymmetry. For the cold season, comfort conditions outside of class A only occur with a radiant asymmetry higher than 10 °C, a condition that was never found during the experiments of the present study. When it comes to global comfort, the analysis revealed that all the glazing systems were capable of assuring an indoor environmental comfort class equal to or higher than class B, without a relevant difference between the four systems. The evaluation of the implications of the different technologies on the thermal comfort perceived by potential occupants has therefore revealed that all the prototypes represent optimal solutions.

4 Conclusion

The research activity presented in this paper deals with the assessment of the thermophysical behaviour, energy, and thermal comfort performance of different responsive envelope components for glazing systems. These systems are based on the adoption of a thermotropic layer (TT) alone, or in combination with a PCM layer (paraffin based, with a melting temperature of 35 °C).

The focus of this paper was the analysis of the heating-season results collected during experiments in an outdoor test cell located in Turin, northwest Italy (Cfa, Köppen climate classification). A methodology based on a double distribution approach was presented for the selection of representative data for performance analysis, before the characterisation of the technologies was carried out, starting with the evaluation of their steady-state, traditional parameters (for example, U value, g-value, and solar and visible transmittance). The results showed that, thanks to the integration in a triple-glazing unit, the insertion of the PCM in the cavity did not significantly decrease the overall thermal resistance of the system. This constitutes a step forward for the development of dynamic glazing systems that make use of PCM. A technology proposed in previous studies (Goia et al., 2014b, 2013) showed promising performance, but also presented some problems related to the increase of thermal losses during the cold season. This issue is solved by the glazing scheme proposed in the present study. The optical and solar properties of the studied glazing – a triple glazing with thermotropic glass and PCM (TGU_TT+PCM) – showed an interesting range of dynamicity during sunny winter days. The solar transmittance varied between 3% for the solid PCM condition and 17% for melted PCM. On the contrary, the results collected on the triple glazing with thermotropic glass (TGU_TT) did not show such a wide range of variation. The most promising results were found during winter days with clear sky, when the dynamic capabilities of the systems were activated. During cloudy days, the energy loss from the TGU_TT+PCM was higher in comparison to the reference TGU due to the reduction of solar heat gain through the PCM. The position of the PCM influenced the performance of the systems during sunny days, with the most promising results registered for the PCM in the outer cavity. This is the configuration that appears to be optimal in terms of responsivity during the heating season. Nevertheless, it has to be remarked that this conclusion is likely to be different in the case of a summer period (when, probably, on the basis of previous research (Goia et al., 2014b), the TGU_TT+PCM(IN) might be better. The integration of PCM with a thermotropic layer enabled a reduction in the energy entering the envelope and the distribution, to some extent, of the solar gains over a longer period. This could lead to an improvement in the energy performance of highly glazed buildings, which present a cooling need also during winter and mid-season as well as in summer.

Finally, a long-term performance analysis demonstrated that the latent heat of the PCM could only be exploited when the PCM was placed in the outer cavity. It was observed that the solar gains were still almost capable of balancing the heat losses, and that the difference, in terms of total energy between the two positions of the PCM-filled cavity during a representative period (18 days) of the heating season, was very small. For all the tested technologies, no thermal discomfort conditions were found.

To summarise, considering the overall results of this experimental campaign, it may be observed that during the heating periods, for the climate conditions of Turin, the dynamic capabilities of the TT and TT+PCM(IN) glazing are activated and exploited to a limited extent.

The TT layer alone does not determine significant improvements; it stays almost always in the "off" state. Moreover, since it produces a decrease in the solar transmittance in comparison to the simple TGU, the consequence is a reduction in the overall solar free gains. With respect to a traditional technology (TGU), its benefit is limited to addressing overheating problems during the central part of sunny days.

The adoption of PCM located in the inner part of the glazing (TGU_TT(IN)) is not beneficial either. The only noteworthy effect of the PCM-IN is represented by a slight improvement in the thermal inertia of the component (sensible heat storage).

Instead, the introduction of the PCM in the outer cavity of the glazing (TGU_TT+PCM(OUT)) is able to make the façade dynamic during those days with clear-sky conditions and can provide a considerable improvement to the thermal and energy behaviour of the system due to the phase transition that occurs. This leads to two positive results: firstly, the problem of the room overheating during the central part of the day is properly addressed; secondly, it allows the shifting of the exploitation of the solar free gains from the sunny hours (when the solar gains are less desirable, or even unwanted) to the late afternoon/evening hours, when the energy demand for heating is higher.

This picture refers to those periods of the year when heating is of concern; given the results obtained from the experimental campaign, it is likely that the conclusions would be exactly reversed (i.e. the PCM-IN configuration would perform more favourably that PCM-OUT) should the summer period be considered. Results related to the cooling season are the object of an experimental campaign that has recently concluded. It is expected that for such conditions the dynamic capabilities provided by the coupling between the TT and PCM layers will find their optimal working conditions and their potential will be fully exploited.

Acknowledgements

The research was started in the framework of “SMARTglass”, a project funded by the Regione Piemonte in 2010 and was part of the activities of the Cost Action 1403 Adaptive Facades Network. The authors would like to thank the Master degree students Alice Raffaelli, Federica Nigro, and Alice Pierleoni for their collaboration and help in the analysis of the experimental data.

References

Allen, K., Connelly, K., Rutherford, P., Wu, Y., 2017. Smart windows—Dynamic control of building energy performance. Energy Build. 139, 535–546. doi:10.1016/j.enbuild.2016.12.093

Baetens, R., Jelle, B.P., Gustavsen, A., 2010. Properties, requirements and possibilities of smart windows for dynamic daylight and solar energy control in buildings: A state-of-the-art review. Sol. Energy Mater. Sol. Cells 94, 87–105. doi:10.1016/j.solmat.2009.08.021

Bianco, L., Goia, F., Serra, V., Zinzi, M., 2015. Thermal and Optical Properties of a Thermotropic Glass Pane: Laboratory and In-Field Characterization. Energy Procedia 78, 116–121. doi:10.1016/j.egypro.2015.11.124

Cuce, E., Riffat, S.B., 2015. A state-of-the-art review on innovative glazing technologies. Renew. Sustain. Energy Rev. 41, 695–714. doi:10.1016/j.rser.2014.08.084

EN, I., 2007. ISO 6946:2007, Building components and building elements -- Thermal resistance and thermal transmittance -- Calculation method.

EN, I., 2005. ISO 7730:2005 Ergonomics of the thermal environment -- Analytical determination and interpretation of thermal comfort using calculation of the PMV and PPD indices and local thermal comfort criteria.

Favoino, F., Overend, M., Jin, Q., 2015. The optimal thermo-optical properties and energy saving potential of adaptive glazing technologies. Appl. Energy 156, 1–15. doi:10.1016/j.apenergy.2015.05.065

Georg, A., Graf, W., Schweiger, D., Wittwer, V., Nitz, P., Wilson, H.R., 1998. Switchable glazing with a large dynamic range in total solar energy transmittance (TSET). Sol. Energy 62, 215–228. doi:10.1016/S0038-092X(98)00014-0

Gladen, A.C., Davidson, J.H., Mantell, S.C., 2014. Selection of thermotropic materials for overheat protection of polymer absorbers. Sol. Energy 104, 42–51. doi:10.1016/j.solener.2013.10.026

Goia, F., Bianco, L., Cascone, Y., Perino, M., Serra, V., 2014a. Experimental Analysis of an Advanced Dynamic Glazing Prototype Integrating PCM and Thermotropic Layers. Energy Procedia 48, 1272–1281. doi:10.1016/j.egypro.2014.02.144

Goia, F., Perino, M., Serra, V., 2014b. Experimental analysis of the energy performance of a full-scale PCM glazing prototype. Sol. Energy 100, 217–233. doi:10.1016/j.solener.2013.12.002

Goia, F., Perino, M., Serra, V., 2013. Improving thermal comfort conditions by means of PCM glazing systems. Energy Build. 60, 442–452. doi:10.1016/j.enbuild.2013.01.029

Goia, F., Zinzi, M., Carnielo, E., Serra, V., 2015. Spectral and angular solar properties of a PCM-filled double glazing unit. Energy Build. 87, 302–312. doi:10.1016/j.enbuild.2014.11.019

Inoue, T., 2003. Solar shading and daylighting by means of autonomous responsive dimming glass: Practical application. Energy Build. 35, 463–471. doi:10.1016/S0378-7788(02)00143-3

Inoue, T., Ichinose, M., Ichikawa, N., 2008. Thermotropic glass with active dimming control for solar shading and daylighting 40, 385–393. doi:10.1016/j.enbuild.2007.03.006

Ismail, K.A.R., Henrı, J.R., 1998. U-values , optical and thermal coefficients of composite glass systems. Sol. Energy Mater. Sol. Cells 52, 155–182. doi:10.1016/S0927-0248(97)00286-9

Li, D., Li, Z., Zheng, Y., Liu, C., Hussein, A.K., Liu, X., 2016a. Thermal performance of a PCM-filled double-glazing unit with different thermophysical parameters of PCM. Sol. Energy 133, 207–220. doi:10.1016/j.solener.2016.03.039

Li, D., Ma, T., Liu, C., Zheng, Y., Wang, Z., Liu, X., 2016b. Thermal performance of a PCM-filled double glazing unit with different optical properties of phase change material. Energy Build. 119, 143–152. doi:10.1016/j.enbuild.2016.03.036

Li, S., Sun, G., Zou, K., Zhang, X., 2016. Experimental research on the dynamic thermal performance of a novel triple-pane building window filled with PCM. Sustain. Cities Soc. 27, 15–22. doi:10.1016/j.scs.2016.08.014

Manz, H., Egolf, P.W., Suter, P., Goetzberger, a., 1997. TIM-PCM external wall system for solar space heating and daylighting. Sol. Energy 61, 369–379. doi:10.1016/S0038-092X(97)00086-8

Muehling, O., Seeboth, A., Haeusler, T., Ruhmann, R., Potechius, E., Vetter, R., 2009. Variable solar control using thermotropic core/shell particles. Sol. Energy Mater. Sol. Cells 93, 1510–1517. doi:10.1016/j.solmat.2009.03.029

Nitz, P., Hartwig, H., 2005. Solar control with thermotropic layers. Sol. Energy 79, 573–582. doi:10.1016/j.solener.2004.12.009

Peel, M.C., Finlayson, B.L., McMahon, T.A., 2007. Updated world map of the Köppen-Geiger climate classification. Hydrol. Earth Syst. Sci. 11, 1633–1644. doi:10.5194/hess-11-1633-2007

Raicu, A., Wilson, H.R., Nitz, P., Platzer, W., Wittwer, V., Jahns, E., 2002. Façade systems with variable solar control using thermotropic polymer blends 72, 31–42. doi:10.1016/S0038-092X(01)00093-7

Seeboth, A., Ruhmann, R., Mühling, O., 2010. Thermotropic and Thermochromic Polymer Based Materials for Adaptive Solar Control. Materials 3, 5143–5168. doi:10.3390/ma3125143

Serra, V., Zanghirella, F., Perino, M., 2010. Experimental evaluation of a climate façade: Energy efficiency and thermal comfort performance. Energy Build. 42, 50–62. doi:10.1016/j.enbuild.2009.07.010

Silva, T., Vicente, R., Rodrigues, F., 2016. Literature review on the use of phase change materials in glazing and shading solutions. Renew. Sustain. Energy Rev. 53, 515–535. doi:10.1016/j.rser.2015.07.201

Weber, A., Resch, K., 2012. Thermotropic glazings for overheating protection. Energy Procedia 30, 471–477. doi:10.1016/j.egypro.2012.11.056

Yao, J., Zhu, N., 2012. Evaluation of indoor thermal environmental, energy and daylighting performance of thermotropic windows. Build. Environ. 49, 283–290. doi:10.1016/j.buildenv.2011.06.004